

Properties of P-vortex and monopole clusters in lattice $SU(2)$ gauge theory

A. V. Kovalenko[†], M. I. Polikarpov[†], S. N. Syritsyn[†] and V. I. Zakharov^{*}

[†] *Institute of Theoretical and Experimental Physics, B. Cheremushkinskaya 25, Moscow, 117259, Russia*

^{*} *Max-Planck Institut für Physik, Föhringer Ring 6, 80805, München, Germany*

ABSTRACT

We study the action and geometry of P-vortices, discriminating between the percolating and finite clusters. We also discuss the interrelation of the monopoles and P-vortices. To define P-vortices we use both the direct maximal center projection and indirect maximal center projection. We find, in particular, that the action density of the P-vortices in short clusters is substantially higher than in the percolating cluster. The surface of the percolating cluster appears random at short distances, with action density depending on the shape.

1 Introduction

The monopole mechanism and P-vortex mechanism are the most popular explanations of the confinement of color [1]. Mostly, these mechanisms are viewed as alternatives. However, at a closer look the field configurations representing monopoles and P-vortices turn to be interrelated [2, 3, 4]. In more detail, the monopole currents form closed lines on 4D lattice, while P-vortices are represented by closed surfaces. The basic observation indicating the unity of the monopoles and vortices is the strong correlation between the monopole trajectories and the vortex surfaces [2, 3, 4].

Moreover, both monopole currents and P-vortices in the confinement phase percolate. In other words, there exists a percolating (infrared, IR) cluster which extends through the whole of the lattice. In the monopole case, it is also well known [5, 6] that apart from the percolating cluster there exist finite (ultraviolet, UV) clusters. Observation of the finite clusters of P-vortices was reported first in [4]. In this note we consider systematically the UV and IR clusters of vortices and monopoles and discuss their interrelation. To check stability of our results against variations in the definition of the P-vortices, we study both the direct maximal center projection (DMCP) [7] and indirect maximal center projection (IMCP) [8]. Preliminary results were presented in [4].

Traditionally, the monopoles and vortices have been considered as effective, infrared degrees of freedom of the YM theories. One of central issues is then, how much dominate these field fluctuations the confining potential. We will contribute to this discussion by presenting new data on the string tension induced by P-vortices, see Sect. 2.

More recently it was realized that the vortices possess highly non-trivial properties in the ultraviolet as well [9]. In particular, it was found [9] that the excess of the full non-Abelian action associated with the P-vortices is ultraviolet divergent at presently available lattices:

$$S_{PV} - S_{vac} \approx 0.54 \frac{A}{a^2} , \quad (1)$$

where A is the area of the vortices, a is the lattice spacing and S_{vac} is the vacuum action. Thus, the probability to find a vortex of area A is suppressed exponentially by the action factor for finite A and $a \rightarrow 0$. Nevertheless it is known [2] that the total area of the P-vortices scales in physical units. The only interpretation of this observation is that the suppression due to the action (1) is balanced by exponential enhancement due to the entropy [9]. Earlier, it was argued [10] that the data [11] indicate a similar cancellation in case of the monopoles.

Thus, monopoles and vortices seem to represent a new kind of vacuum fluctuations which exhibit both ultraviolet and infrared scales, lattice spacing a and Λ_{QCD} , respectively. They can be called selftuned since the action and entropy factors seem to cancel to a high degree of accuracy without tuning any external parameter. This by itself justifies as detailed study of the branes¹ as possible. In a way, this field theoretic facet of the branes can be addressed even without reference to the confinement. In particular, the branes might shed light on the dual formulation of the Yang-Mills theories [12].

Motivated by these considerations, we undertake here a detailed study of the action associated with the vortices and of their geometry, the line of investigation suggested by [9]. In particular, to have an exponentially enhanced entropy, the surface should be random on the scale of the lattice spacing a . Hence, our interest is in the local geometry of the P-vortices. A new point compared to [9] is that we study the infinite and finite clusters separately. In Sect. 3 we present results on geometrical characteristics of the P-vortices. Sect. 4 is devoted to the results on their action. The main definitions and details of numerical calculations are given in the Appendix while Sect. 5 is conclusions.

2 $Z(2)$ string tension

It is well known that monopoles in the maximal Abelian projection are responsible for about 90% of the string tension both in $SU(2)$ gluodynamics [13] and in lattice QCD with two dynamical quarks [14]. There has been a long discussion in the literature on whether the P-vortices reproduce well the non-Abelian string tension (see Refs. [8], [15], [16], [17] and references therein). On Fig. 1 we show the ratio of the $Z(2)$ string tension obtained from $Z(2)$ links and the full $SU(2)$ string tension. To calculate the $Z(2)$ string

¹By branes we mean the (infinitely) thin vortices which carry the action (1) and which are populated with the monopoles.

tension we use the standard Creutz ratio for loops up to 7×7 lattice spacings (for all values of β). It appears that near the continuum limit for IMCP and DMCP $\sigma_{Z(2)}/\sigma_{SU(2)}$ is of the order of 0.6. Probably to reproduce the full string tension from $Z(2)$ variables we have to use some other $Z(2)$ projection [16]. In any case the fact that we reproduce a substantial part of the string tension from $Z(2)$ variables shows that P-vortices even in the considered projections are related to the confinement.

3 Geometry of P-vortices

3.1 Randomness of the surfaces

As is mentioned in the Introduction the selftuning of the P-vortices assumes randomness of their surfaces at the scale of the lattice spacing a . Our main point now is that the randomness can be probed through measurements. Let us discuss first how “random” is the surface formed by the IR P-vortex cluster. The plaquettes forming a surface can have the junction configurations shown in Fig. 2. Junctions of 2 plaquettes, can be “plain” or “bend”. For a random surface in D=4 we have:

$$\frac{N_{plain}}{N_{bend}} = \frac{1}{4}. \quad (2)$$

If self-intersections are rare, $N_{SI}, N_{Bent SI} \ll N_{link}$ (N_{link} is the total number of links on the surface), then

$$N_{plain} = \frac{1}{5}N_{link}, \quad N_{bend} = \frac{4}{5}N_{link}. \quad (3)$$

We find out that the relations (2) and (3) are satisfied to a good accuracy for IR clusters in a wide region of the lattice spacing, a . This is shown in Fig. 3 for IMCP, for DMCP the results are very similar. Thus, IR clusters at short distances behave like random surfaces. Relation (3) is also satisfied to a good accuracy since the number of links with self intersections of P-vortices is small ($\approx 3.4\%$ for IMCP and $\approx 2.7\%$ for DMCP for the largest value of $a = 0.139 fm$, and even less for smaller values of the lattice spacing).

The ultraviolet (UV), or finite, clusters have quite different geometry. They are dominated by small objects like $1 \times 1 \times 1$, $1 \times 1 \times 2$ and so on (see Fig. 4 and sect. 3.2). For all considered lattice spacings most of plaquette junctions on UV P-vortices clusters are “bend” (more than 95.5% for IMCP and 96.4% for DMCP). The number of other plaquette junctions also weakly depends on the lattice spacing.

3.2 Spectrum of finite P-vortex clusters

One of the basic geometric characteristics of the P-vortices is their total area. It is known to scale in physical units [7, 9]:

$$A_{vort} \approx 24 fm^{-2} \cdot V_4, \quad (4)$$

where V_4 is the volume of the lattice in fm^4 . The area (4) includes both IR and UV clusters.

Table 1: Values of the parameter τ

β	$\log A_{max}$	τ
IMCP		
2.40	4.5	3.24 ± 0.05
2.50	5.5	3.14 ± 0.04
2.60	6.0	3.24 ± 0.04
DMCP		
2.40	5.5	3.36 ± 0.06
2.50	6.0	3.49 ± 0.06
2.60	6.0	3.85 ± 0.09

Consider now the spectrum of the UV clusters. On Fig. 4 the number of UV clusters of the given area A (lattice units) is shown in logarithmic scale for IMCP. Three values of β are used: $\beta = 2.40$, $\beta = 2.50$, $\beta = 2.60$. The fit of the spectrum by the expression

$$N(A) \sim \frac{1}{A^\tau}, \quad (5)$$

is shown by solid lines. The results of the fit are given in the Table 1, it is seen that $\tau \approx 3$ for IMCP. Performing the fit we neglect the smallest clusters (cubes with $A = 6$), since they reflect the geometry of the lattice.

To summarize, the density of the UV clusters reveals a strong dependence on the lattice spacing a^2 . This strong dependence so far was consistent with the a independence of the total area (4). Extrapolation to smaller a seems, however, non-trivial. Either (4) or the exponential in (5) is to be changed at smaller lattice spacings.

3.3 P-vortices and monopoles

In Refs. [2] it was shown that at $\beta = 2.4$ the main part of the monopole trajectories extracted in the maximal Abelian projection lie on P-vortices in IMCP. Below we show that this result is valid in a wide range of the lattice spacing. Moreover we consider separately IR and UV clusters of monopoles and P-vortices. In Figs. 5, 6 we present the densities of IR and UV monopole clusters lying on IR and UV P-vortices in IMCP. We also show the densities of IR and UV monopole clusters which do not belong to P-vortices (“free” monopoles). We see that the density of IR monopoles lying on IR P-vortices is much larger than other densities. Similarly, the density of UV monopoles is mainly due to monopoles lying on UV P-vortices. This density is divergent as $1/a$ at small values of a . The fit of four points at small values of a by the function $C_1 + C_2/a$ gives:

$$C_1 \approx -8.5(2)fm^{-3}, \quad C_2 \approx 1.19(1)fm^{-2} \quad (6)$$

For DMCP we observe similar correlations of monopoles and P-vortices.

²The average area of UV clusters is $\langle A \rangle = \int_a^\infty N(A)A dA \approx \frac{C}{a^2}$

4 Action density of P-vortices

4.1 Percolating cluster vs finite clusters

As we have mentioned in the Introduction the average action associated with the P-vortices is ultraviolet divergent, with a simple a dependence, see (1). However, in case of the monopoles there exists also a finer effect. Namely, the monopole action for finite (UV) clusters is somewhat higher than for the percolating (IR) cluster [11]. The result emphasizes the physical nature of the lattice monopoles since it is natural that the percolating monopoles have lower action.

In this section we report on observation of a similar effect in case of the P-vortices. Namely, in Fig. 7 we plot the excess of the action, $S_{PV} - S_{vac}$ vs. lattice spacing a . The vacuum action density is defined in the usual way, $S_{vac} = \beta < 1 - \frac{1}{2}\text{Tr}U_P >$, S_{PV} is the same action but only for plaquettes dual to P-vortices. The non-Abelian action density on the plaquettes dual to plaquettes belonging to all P-vortices seems to be constant in lattice units. In other words it is divergent in physical units as $a \rightarrow 0$. The action for IR clusters is very close for IMCP and DMCP, while the action for UV clusters is larger for DMCP.

4.2 Action vs local P-vortex geometry

As mentioned in the Introduction, P-vortices appear to exhibit tuning of the action and entropy. From theoretical point of view the very existence of such a surface is a highly non-trivial and challenging observation. The point is that such tuning is not possible in case of the Nambu-Goto action. Thus, one can expect that action is actually not uniform but depends on the local geometry.

To study possible relation between the local geometry and action we have measured dependence of the action on the type of the junction of neighboring plaquettes. On Fig. 8 we show the excess of the average plaquette action on the plaquettes which are attached to the link in a special manner (see Fig. 2) for IMCP. For DMCP we have analogous results. The data do indicate that the ‘plain’ junction costs less action than the bended ones. The tendency is especially clearly manifested in case of the IR vortices.

4.3 P-vortex geometry and monopoles

Thus, the most part of the monopole currents lie on the links which belong to P-vortices, and now we discuss the correlation of the different types of the plaquette junctions on P-vortex (see Fig. 2) with the monopole currents. On Fig. 9 we show for IMCP the ratio $\frac{N_{link,mon}^k}{N_{link}^k}$, where N_{link}^k is the average number of the links corresponding to the junction k , $N_{link,mon}^k$ is the number of links which carry monopole current and correspond to the junction k . In case of DMCP, we have very similar results.

5 Conclusions

In this note we have presented detailed measurements of action and local geometrical characteristics of P-vortices and their correlations with monopoles. All the measurements are done separately for the percolating and finite clusters. The results obtained for DMCP and IMCP are very similar.

It is worth emphasizing that all the characteristics we have been considering are gauge invariant. Indeed, we have measured the full non-Abelian action associated with the branes (P-vortices). Also, the geometrical characteristics are in the physical units, or in units of Λ_{QCD}^{-1} . On the other hand, the branes themselves are defined within a particular projection and the definition is not unique. To reconcile these observations one is invited to assume that through the projection one detects actually gauge invariant objects. Then various projections are not necessarily the same effective to detect these gauge invariant vacuum fluctuations. The criterion which worked empirically so far is that the projections which are most effective to describe the confining potential exhibit gauge invariant properties in the most regular way.

Our detailed measurements did not change this picture in its basic points. However, in quite a few cases we found substantial differences between the properties of percolating and finite clusters of P-vortices. In particular, it is only the surface of the percolating cluster which exhibits the randomness on the scale of the lattice spacing a (which is a prerequisite for cancellation between the huge action and entropy factors). The small clusters are dominated by elementary cubes. One is inclined to consider such clusters as artifacts.

On the other hand, the total area of the infrared cluster alone does not scale so beautifully as the total area of all the P-vortices. Also, the non-Abelian action associated with the ultraviolet clusters of P-vortices is considerably higher than the action for the percolating cluster. Which suggests that the vortices are physical. Measurements at smaller a are desired to distinguish between facts and artifacts in case of the ultraviolet clusters.

One of our results is the spectrum of the ultraviolet clusters in IMCP as a function of their area A ,

$$N(A) \sim A^{-3}$$

If the theory of the vortices were known, the spectrum were predictable. This is true, in particular, in case of the monopoles, see the second paper in Ref. [10]. At the moment, however, the theory of the percolating surfaces is not known yet.

We have confirmed strong correlation between the monopoles and the P-vortices. Moreover, we have observed that the infrared monopoles are correlated mostly with the percolating cluster of P-vortices. The investigation of the properties of the IR monopole clusters in 4D SU(2) lattice gauge theory allow to conclude that monopoles percolate on two dimensional surfaces [12].

Detailed studies of the action of the P-vortices indicate dependence of the action on the local geometry. Also, the monopole trajectories belonging to the vortices are having a larger excess of the action than the vortices on average. On the theoretical side, this observation is rather gratifying although cannot be fully interpreted at present. Indeed,

it is known (see, e.g., [18]) that the tuning between action and entropy is not possible at all for the simplest (Nambu-Goto) action,

$$S = \sigma \cdot A.$$

Our results indicate that the action should include terms related to the curvature of the surface and monopole trajectories. Both modifications of the simplest action above have been considered on various occasions in the literature. In particular, the action of the particles living on submanifolds is commonly introduced in theory of D-branes, for review and references see, e.g., [19]. Theories with action depending on the curvature have been widely discussed in quantum geometry, for review and references see, e.g. [18]. Application of the latter idea to the P-vortices was considered first in Ref. [20].

At present, there is no theory of P-vortices on the fundamental level. Hopefully, the results on the action and geometry of the vortices obtained in this paper would allow to narrow the search for such a theory.

Acknowledgements

A.V.K., M.I.P. and S.N.S. are partially supported by grants RFBR 02-02-17308, RFBR 01-02-17456, DFG-RFBR 436 RUS 113/739/0, INTAS-00-00111, and CRDF award RPI-2364-MO-02; V.I.Z. is partially supported by INTAS-00-00111 grant.

The authors are grateful to V.G. Bornyakov and J. Greensite for useful discussions.

Appendix

To define the P-vortices we use both the DMC [7] and the IMC [8] projections. The DMCP in SU(2) lattice gauge theory is defined by the maximization of the functional

$$F_1(U) = \sum_{n,\mu} (\text{Tr} U_{n,\mu})^2, \quad (7)$$

with respect to gauge transformations, $U_{n,\mu}$ is the lattice gauge field. The maximization of (7) fixes the gauge up to Z(2) gauge transformations and the corresponding Z(2) gauge field is defined as: $Z_{n,\mu} = \text{sign Tr} U_{n,\mu}$. The plaquettes $Z_{n,\mu\nu}$ constructed as product of links $Z_{n,\mu}$ along the border of the plaquette have values ± 1 . The P-vortices (forming closed surfaces in 4D space) are made from the plaquettes, dual to plaquettes with $Z_{n,\mu\nu} = -1$.

To get IMCP we first fix the maximally Abelian gauge by maximizing the functional

$$F_2(U) = \sum_{n,\mu} \text{Tr} (U_{n,\mu} \sigma_3 U_{n,\mu}^+ \sigma_3), \quad (8)$$

with respect to gauge transformations. This procedure leaves unfixed $U(1)$ degrees of freedom, the corresponding $U(1)$ compact gauge field is $e^{i\theta_{n,\mu}}$, $\theta_{n,\mu}$ being the phase of the $(1, 1)$ element of the link matrix $U_{n,\mu}$. After that we can extract monopole currents

Table 2: Parameters of configurations.

β	Size	N_{IMCP}	N_{DMCP}
2.35	16^4	20	20
2.40	24^4	50	20
2.45	24^4	20	20
2.50	24^4	50	20
2.55	28^4	37	17
2.60	28^4	50	20

from the Abelian fields. Finally, we project gauge degrees of freedom $U(1) \rightarrow Z(2)$ by the procedure analogous to the DMCP case. We substitute into eq. (7) the Abelian matrix: $U_{n,\mu} \rightarrow U_{n,\mu}^{Ab} \equiv \text{diag}(e^{i\theta_{n,\mu}}, e^{-i\theta_{n,\mu}})$ and maximize $F_1(U)$ with respect to $U(1)$ gauge transformations.

We work at various lattice spacings to check the existence of the continuum limit of our observables. The parameters of our gauge field configurations are listed in Table 2. To fix the physical scale we use the string tension in lattice units [21], $\sqrt{\sigma} = 440 \text{ MeV}$.

To fix the maximally Abelian gauge and maximal center gauge we create 20 randomly gauge transformed copies of the gauge field configuration and apply the Simulated Annealing [13, 17] algorithm to each copy. We use in calculations that copy which correspond to the maximal value of the gauge fixing functional. To fix the indirect maximal center gauge from configuration fixed to maximally Abelian gauge one gauge copy is enough to work with our accuracy.

References

- [1] M.N. Chernodub, M.I. Polikarpov, in *'Cambridge 1997, Confinement, duality, and nonperturbative aspects of QCD'*, p. 387; [hep-th/9710205](#);
J. Greensite, *Prog. Part. Nucl. Phys.* **51**, 1 (2003), [hep-lat/0301023](#)
- [2] L. Del Debbio, M. Faber, J. Greensite, S. Olejnik, in *'Zakopane 1997, New developments in quantum field theory'*, p. 47, [hep-lat/9708023](#);
J. Ambjorn, J. Giedt, J. Greensite, *JHEP* **0002**, 033 (2000).
- [3] P. de Forcrand, M. Pepe, *Nucl. Phys.* **B598**, 557 (2001).
- [4] A. V. Kovalenko, M. I. Polikarpov, S. N. Syritsyn and V. I. Zakharov, *"Interplay of monopoles and P-vortices"*, preprint ITEP-LAT/2003-23, [hep-lat/0309032](#).
- [5] A. Hart and M. Teper, *Phys. Rev.* D58, 014504 (1998).
- [6] V.G. Bornyakov, P.Yu. Boyko, M.I. Polikarpov and V.I. Zakharov, *Nucl. Phys.* **B672** 222 (2003).

- [7] L. Del Debbio, M. Faber, J. Giedt, J. Greensite and S. Olejnik, *Phys.Rev.* **D58**, 094501 (1998).
- [8] L. Del Debbio, M. Faber, J. Greensite, S. Olejnik, *Phys. Rev.* **D55**, 2298 (1997).
- [9] F. V. Gubarev, A. V. Kovalenko, M. I. Polikarpov, S. N. Syritsyn and V. I. Zakharov, *Phys. Lett.* **B574**, 136 (2003).
- [10] V. I. Zakharov, “*Hidden mass hierarchy in QCD*”, [hep-ph/0204040](#);
M. N. Chernodub and V. I. Zakharov, *Nucl. Phys.* **B669**, 233 (2003).
- [11] V. G. Bornyakov, M. N. Chernodub, F. V. Gubarev, M. I. Polikarpov, T. Suzuki, A. I. Veselov and V. I. Zakharov, *Phys. Lett.* **B537**, 291 (2002).
- [12] V. I. Zakharov, “*Hints on dual variables from the lattice $SU(2)$ gluodynamics*”, [hep-ph/0309301](#).
- [13] G. S. Bali, V. Bornyakov, M. Muller-Preussker and K. Schilling, *Phys. Rev.* **D54**, 2863 (1996).
- [14] DIK Collaboration (V. G. Bornyakov et al.), “*Dynamics of monopoles and flux tubes in two flavor dynamical QCD*”, [hep-lat/0310011](#).
- [15] T. G. Kovacs and E. T. Tomboulis, *Phys. Lett.* **B463**, 104 (1999).
- [16] M. Faber, J. Greensite and S. Olejnik, *Phys. Rev.* **D64**, 034511 (2001).
- [17] V. G. Bornyakov, D. A. Komarov and M. I. Polikarpov, *Phys. Lett.* **B497** 151 (2001);
V. G. Bornyakov, D. A. Komarov, M. I. Polikarpov and A. I. Veselov, in ‘Osaka 2000, “*Quantum chromodynamics and color confinement*”, p.133’, [hep-lat/0210047](#).
- [18] J. Ambjorn, “*Quantization of geometry*”, [hep-th/9411179](#).
- [19] C. V. Johnson, “*D-Branes*”, Cambridge monographs on mathematical physics, Cambridge (2003).
- [20] M. Engelhardt, H. Reinhardt, *Nucl.Phys.* **B585**, 591 (2000).
- [21] J. Fingberg, U. M. Heller and F. Karsch, *Nucl. Phys.* **B392**, 493 (1993).

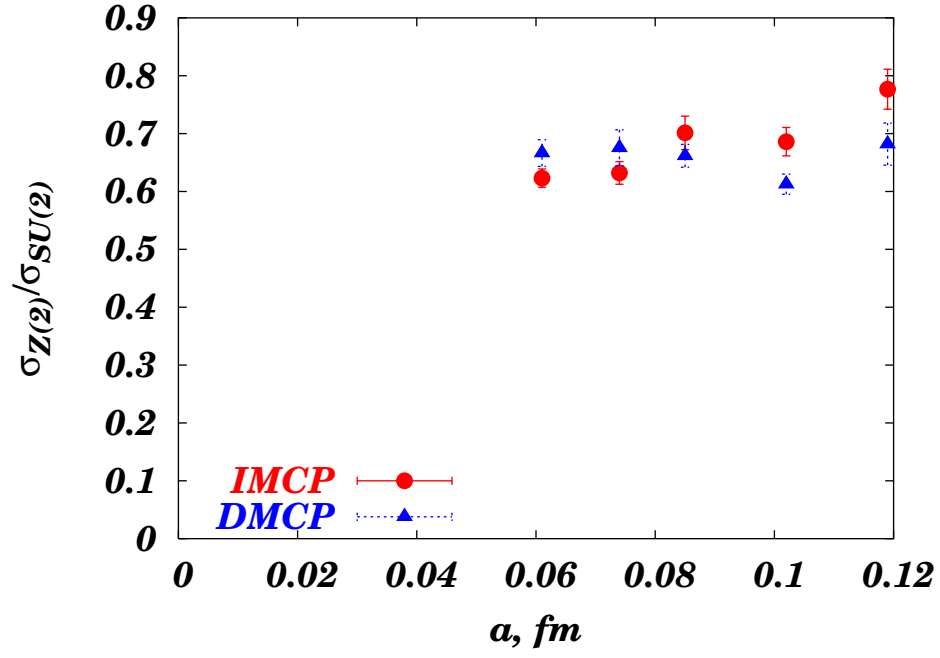


Figure 1: The ratio of the $Z(2)$ string tension and the full $SU(2)$ string tension for IMCP and for DMCP.

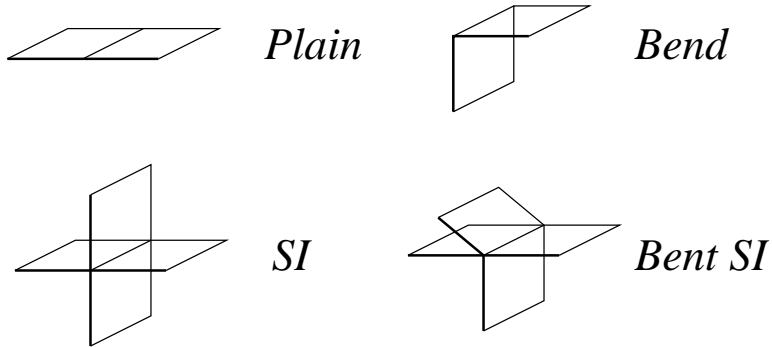


Figure 2: Possible two and four plaquette junctions in $D=4$. Junctions of six plaquettes are very rare, and we do not consider them.

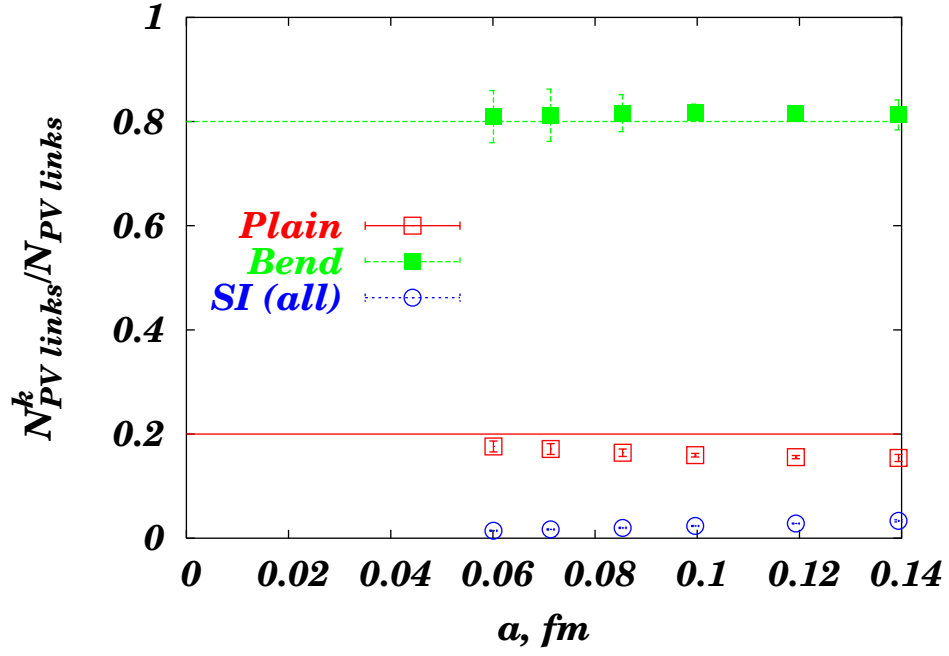


Figure 3: Probability of different types of junctions on the IR P-vortices for IMCP.

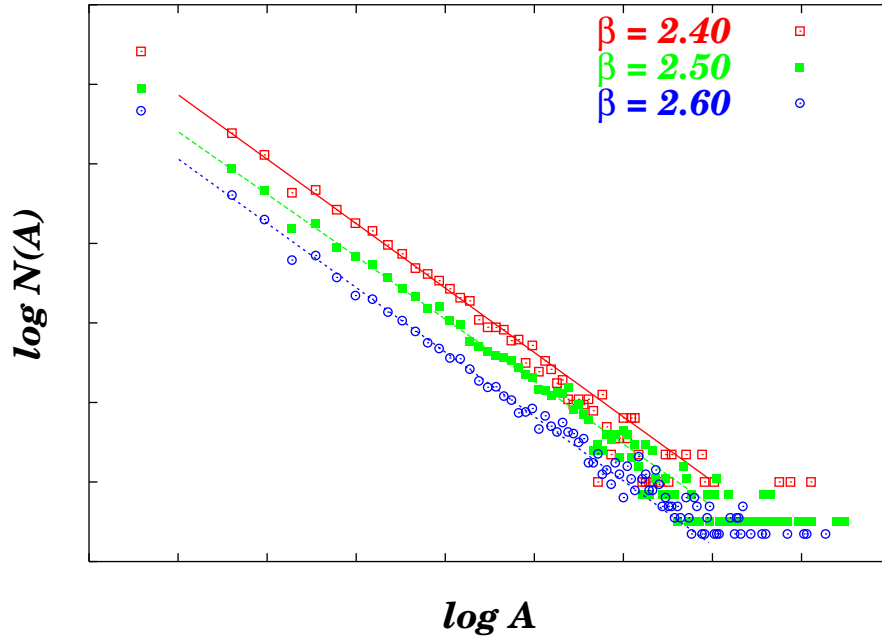


Figure 4: UV P-vortex cluster spectrum in IMCP. Displacement in "y"-axis is made for convenience.

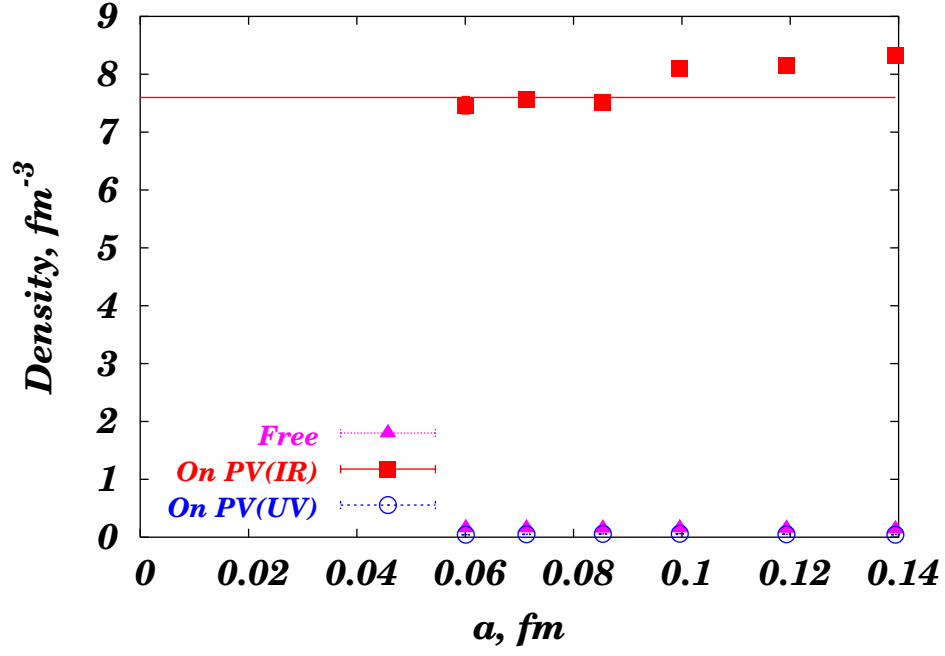


Figure 5: Density of IR monopole currents.

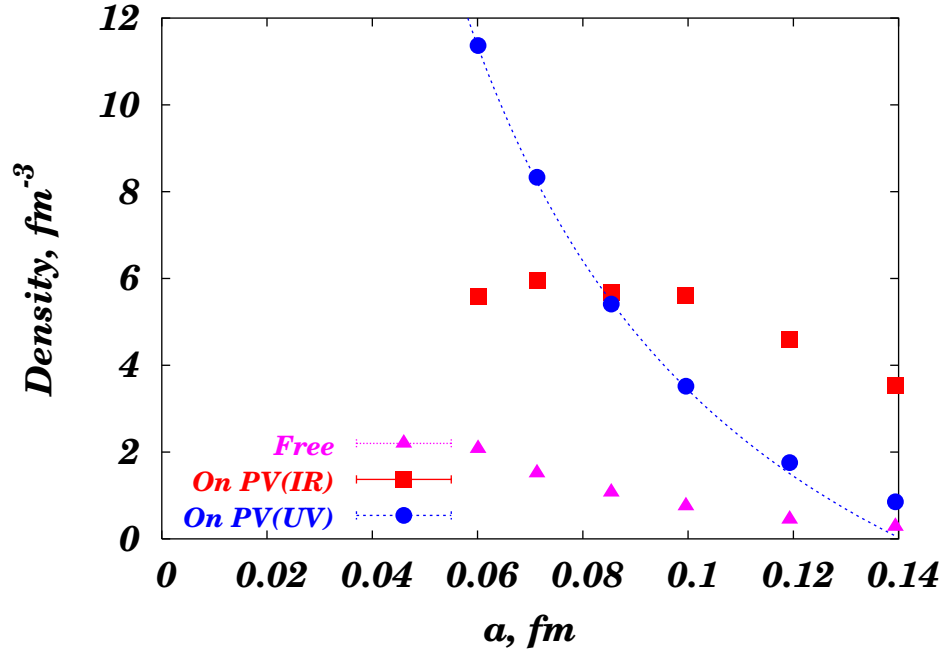


Figure 6: Density of UV monopole currents.

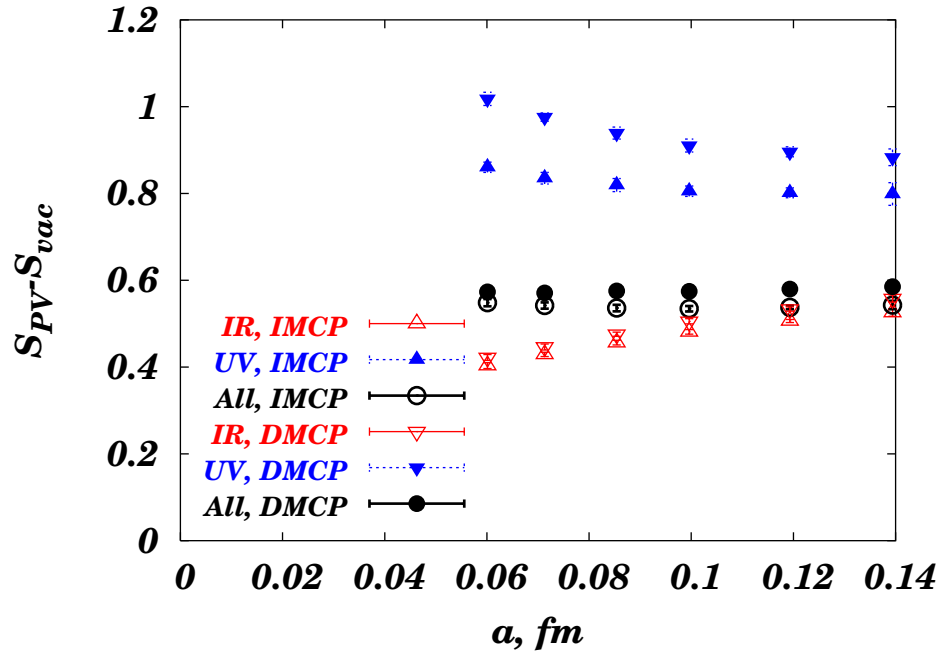


Figure 7: Excess of the plaquette action density on the plaquettes dual to plaquettes belonging to P-vortices for IMCP and DMCP.

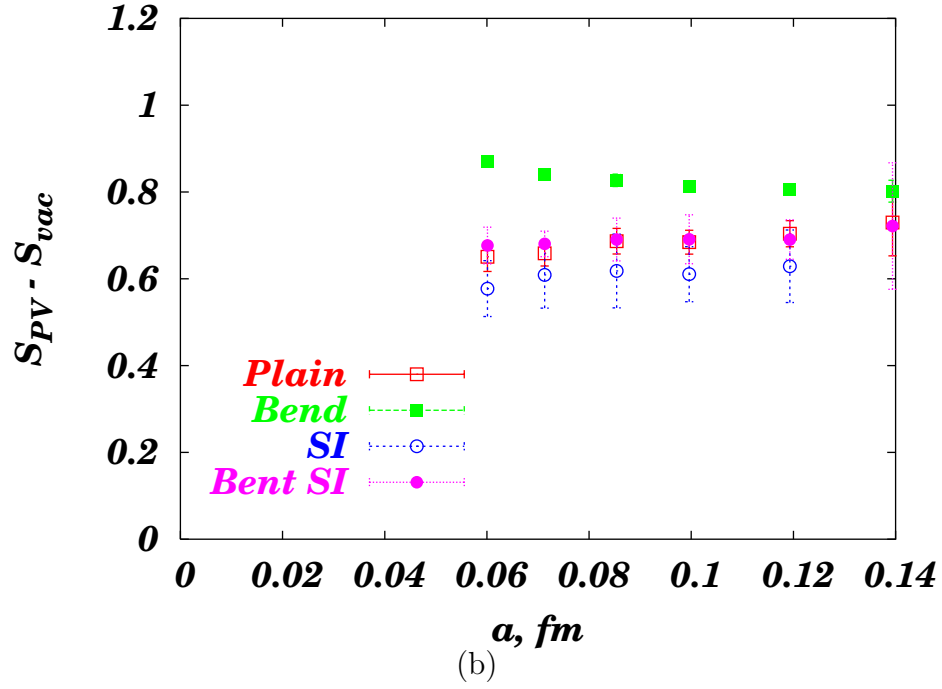
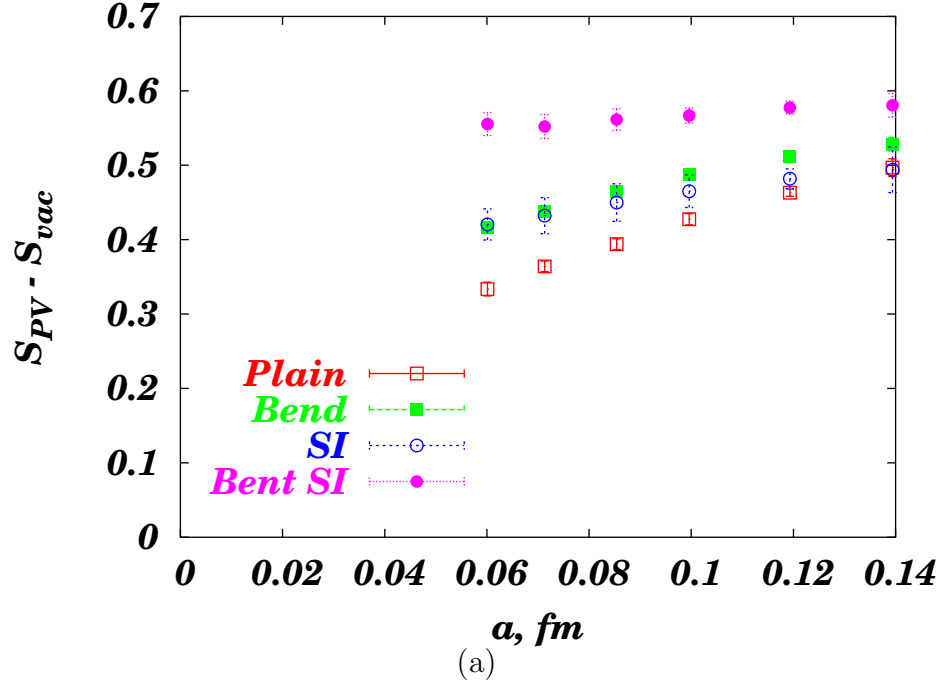


Figure 8: Dependence of the excess of the plaquette action on the local geometry of P-vortex cluster for IMCP for various lattice spacings; (a) IR cluster, (b) UV cluster.

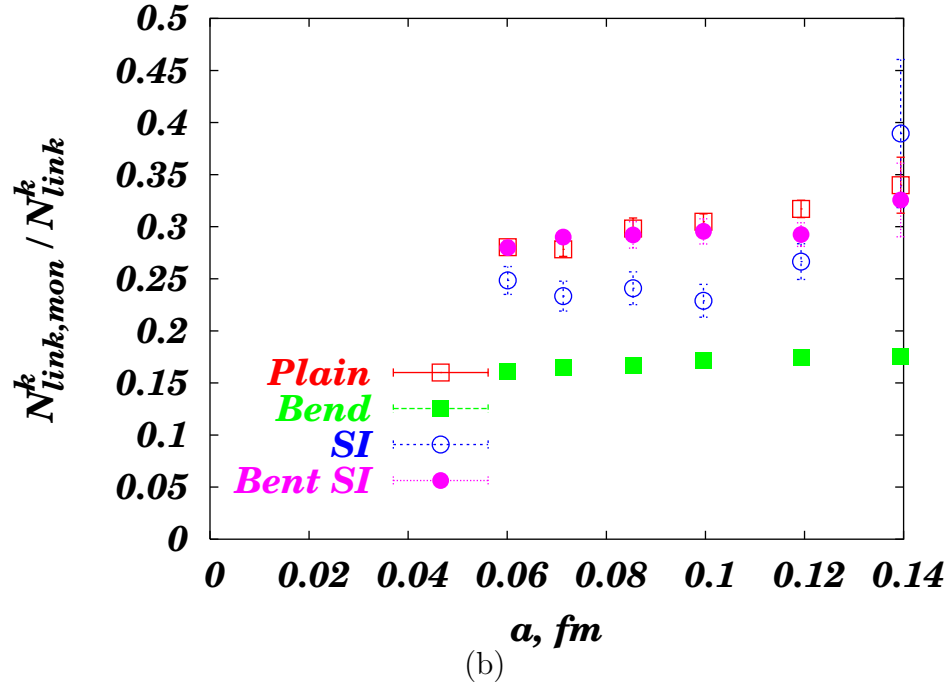
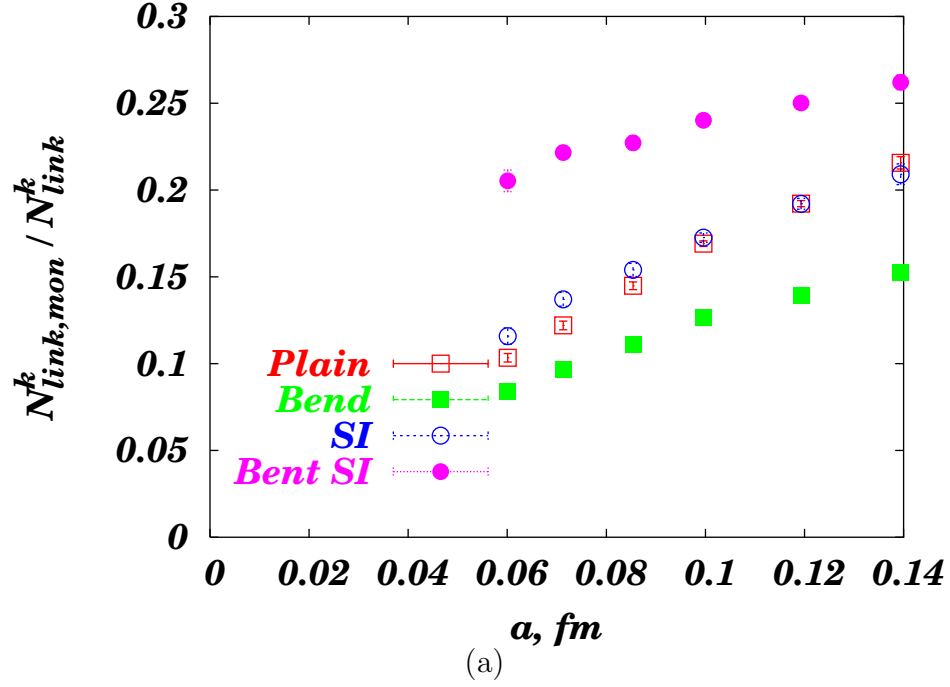


Figure 9: Ratio of number of links with monopoles and number of all links of certain junction type for IMCP P-vortices; (a) IR cluster, (b) UV cluster.